ASSOCIATED PRODUCTION AND DECAY OF NEUTRALINOS AND SELECTRONS IN $e^-\gamma$ COLLISIONS *

C. BLÖCHINGER AND H. FRAAS

Institut für Theoretische Physik, Universität Würzburg
e-mail: bloechi@physik.uni-wuerzburg.de
e-mail: fraas@physik.uni-wuerzburg.de

(Received November 3, 1997)

In the framework of the Minimal Supersymmetric Standard Model (MSSM) with R-parity conservation, angular distributions and total cross sections for the process $e^-\gamma \longrightarrow \tilde{\chi}_1^0 \tilde{e}_{L/R} \longrightarrow \tilde{\chi}_1^0 \tilde{\chi}_1^0 e^-$ are presented in the $e^-\gamma$-cms and the e^-e^+-cms of a photon linear collider (PLC) with CMS-energy $\sqrt{s} = 500$ GeV.

PACS numbers: 11.30. Pb, 13.88. +3, 14.80. Ly

1. Introduction

In the search for heavy selectrons the associated production of a selectron and a gaugino-like LSP $\tilde{\chi}_1^0$ is favoured compared with selectron pair production in e^+e^--annihilation because of the lower threshold energy. Therefore the PLC would be a good facility for selectron search.

2. MSSM parameters and scenarios

The interaction eigenstate of the neutralino $\tilde{\chi}_1^0$ is a mixing of the photino $\tilde{\gamma}$, the zino $\tilde{Z}$ and the higgsino $\tilde{H}_a^0$, $\tilde{H}_b^0$ weak eigenstates. Its mass and mixing character depends on the SU(2) gaugino mass parameter M,the higgsino mass parameter μ and the ratio $\tan\beta = \frac{v_2}{v_1}$ of the two vacuum expectation values of the higgsinos [1].

We have chosen three representative scenarios with $\tan\beta = 2$ and different mixing character of the LSP (Table I).

* Presented by Claus Blöchinger at the XXI School of Theoretical Physics "Recent Progress in Theory and Phenomenology of Fundamental Interactions", Ustroń, Poland, September 19–24, 1997.

TABLE I

Masses and mixing characters of the LSP $\tilde{\chi}_1^0 = N_{11}\tilde{\gamma} + N_{12}\tilde{Z} + N_{13}\tilde{H}_a^0 + N_{14}\tilde{H}_b^0$ in the different scenarios.

	M/GeV	μ/GeV	$m_{\tilde{\chi}_1^0}$/GeV	N_{11}	N_{12}	N_{13}	N_{14}
A	73.16	-219.47	40.0	-0.9477	+0.2994	+0.0795	+0.0772
B	169.52	+155.04	54.1	-0.4766	+0.6639	-0.5108	-0.2668
C	218.93	-72.96	67.3	-0.1304	+0.1887	-0.1952	+0.9536

For the values $m_0 = 50/200$ GeV of the common scalar mass parameter at the GUT-scale, one obtains the selectron masses from the Polchinski-equation [2]. They are listed in Table II.

TABLE II

Selectron masses in the different scenarios for $m_0 = 50/200$ GeV.

	$m_{\tilde{e_L}}$/GeV	$m_{\tilde{e_R}}$/GeV
A	89.9/213.5	69.8/205.9
B	162.9/253.1	101.3/218.5
C	204.2/281.4	121.1/228.4

3. Analytical calculation of the cross section

The amplitude for $e^- + \gamma \longrightarrow \tilde{\chi}_1^0 + \tilde{e}_{L/R}$ contains contributions of the exchange of an electron in the direct channel and selectrons in the crossed channel.

We consider only the direct leptonic decay $\tilde{e}_{L/R} \longrightarrow \tilde{\chi}_1^0 + e^-$. The cross section for the combined process factorizes in the differential production cross section $d\sigma_P$ and and the differential decay width $d\Gamma_S$. In the narrow-width-approximation for the decaying selectron, one gets the simple result:

$$d\sigma = \frac{E_{\tilde{e}_{L/R}}}{|m_{\tilde{e}_{L/R}}|\Gamma_S} d\sigma_P d\Gamma_S \,. \tag{1}$$

To obtain the cross sections in the e^+e^- cms of the PLC, one has to fold the cross sections in the $e^-\gamma$ cms with the energy distribution of the Compton-backscattered laser photons. For more details, see [3].

4. Numerical results

4.1. Angular distributions in the $e^-\gamma$ cms

Since in the production process only the photino and zino components of the neutralinos contribute, the cross section for scenario A is the highest. The shape of the angular distributions is very similar in scenarios B and C. It is however by a factor of 10 and 1000 lower than in scenario A. Therefore, in Figs 1 and 2, we only present our results for scenario A for unpolarized as well as for left and right circularly polarized photons. (θ is the angle between the incoming and the outgoing electron)

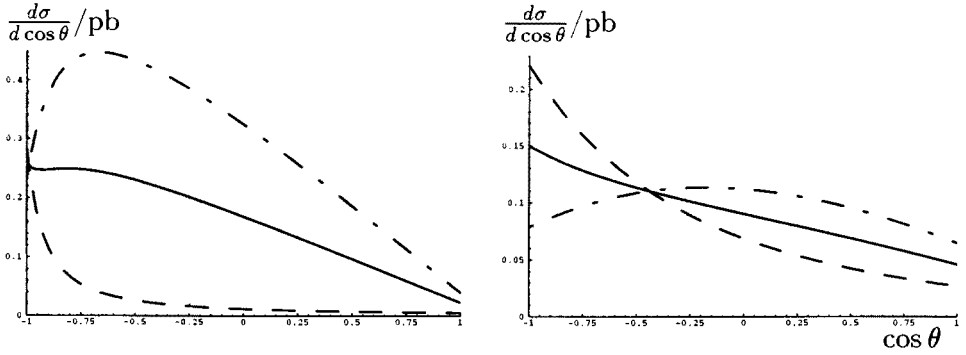

Fig. 1. Angular distribution of the electron from the process $e^-\gamma \longrightarrow \tilde{\chi}_1^0 \tilde{e}_R \longrightarrow e^- + \not{E}$ in scenario A, $m_0 = 50$ GeV (left) and $m_0 = 200$ GeV (right), —— = unpolarized, — — — = right circularly polarized, — · — · – = left circularly polarized photons.

The shape of the angular distributions sensitively depends on the photon polarization. For $m = 50$ GeV the electron prefers the backward hemisphere for unpolarized as well as for circularly polarized photons. This is most pronounced for the case of $\tilde{e_R}$ ($\tilde{e_L}$) and right (left) circularly polarized photons. For $m = 200$ GeV, however, the angular distribution is nearly forward-backward symmetric for $\tilde{e_R}$ ($\tilde{e_L}$) and left (right) circularly polarized photons.

Since $m_{\tilde{e_R}} < m_{\tilde{e_L}}$ [2] the cross sections for left-handed selectrons are always lower than those for right-handed selectrons.

4.2. Angular distribution in the e^-e^+ cms

In Figs. 3 and 4 we compare the folded and the unfolded angular distributions in scenario A for $\sqrt{s}_{e\gamma} = 500$ GeV and $\sqrt{s}_{ee} = 500$ GeV for

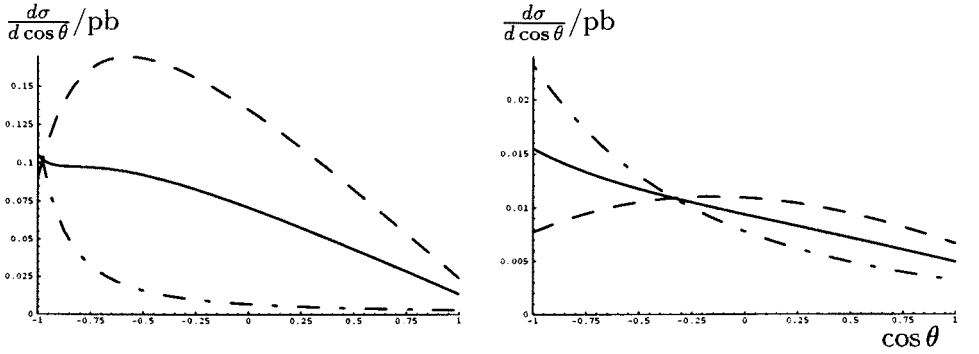

Fig. 2. Angular distribution of the electron from the process $e^-\gamma \longrightarrow \tilde{\chi}_1^0\tilde{e}_L \longrightarrow e^- + \not{E}$ in scenario A, $m_0 = 50$ GeV (left) and $m_0 = 200$ GeV (right), —— = unpolarized, — — — = right circularly polarized, — · — · – = left circularly polarized photons.

unpolarized photons. In which angular region the folded cross section is higher or lower than the unfolded one, sensitively depends on the interplay between the energy and helicity distribution of the backscattered photons and on the value of m_0.

Again the distributions for scenario B and C are much smaller but have the same shape, so that they are not presented here.

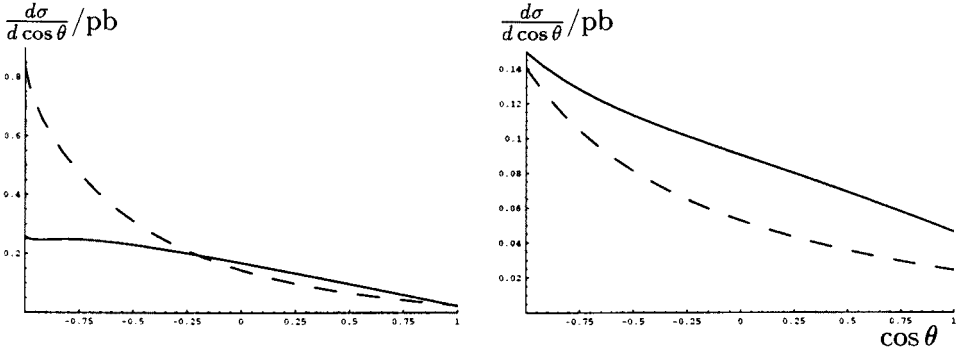

Fig. 3. Angular distribution of the electron from the process $e^-\gamma \longrightarrow \tilde{\chi}_1^0\tilde{e}_R \longrightarrow e^- + \not{E}$ in the $e\gamma$ and the ee CMS, scenario A, $m_0 = 50$ GeV (left) and $m_0 = 200$ GeV (right), —— = unfolded, — — — = folded cross sections.

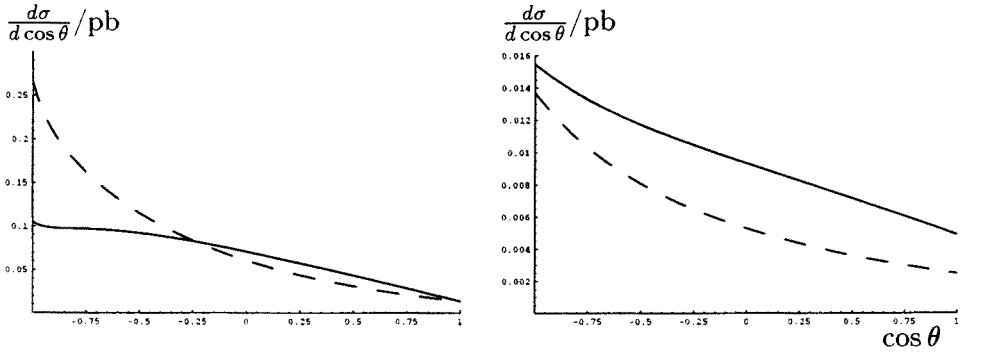

Fig. 4. Angular distribution of the electron from the process $e^-\gamma \longrightarrow \tilde{\chi}_1^0\tilde{e}_L \longrightarrow e^- + \not{E}$ in the $e\gamma$ and the ee CMS, scenario A, $m_0 = 50$ GeV (left) and $m_0 = 200$ GeV (right), —— = unfolded, — — — = folded cross sections.

4.3. Total Cross Section in the $e^-\gamma$ cms

In Fig. 5 we present the total cross sections for circularly polarized and unpolarized photons in scenario A with $m_0 = 50$ GeV. All other total cross sections again have a similar shape, but are much smaller.

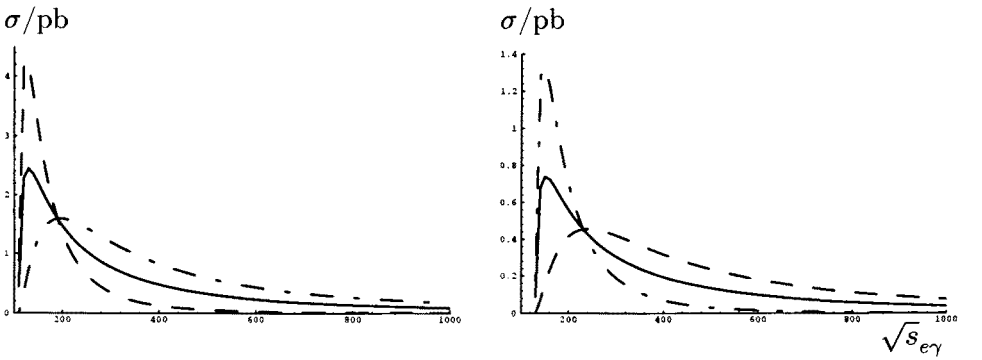

Fig. 5. Total cross section of the processes $e^-\gamma \longrightarrow \tilde{\chi}_1^0\tilde{e}_R \longrightarrow e^- + \not{E}$ (left) and $e^-\gamma \longrightarrow \tilde{\chi}_1^0\tilde{e}_L \longrightarrow e^- + \not{E}$ (right) in scenario A, $m_0 = 50$ GeV, —— = unpolarized, — — — = right circular polarized, — · — · – = left circular polarized photons.

5. Conclusion

We have computed the electron angular distribution from associated production $e^-\gamma \longrightarrow \tilde{\chi}_1^0 \tilde{e}_{L/R}$ and the direct leptonic decay of the selectron. Numerical results are given for both a monochromatic, unpolarized or polarized photon beam and for a PLC. For a monochromatic photon beam the shape of the cross sections sensitively depends on the photon polarization. For small values of m_0 most of the electrons go in the backward region, whereas for higher values of m_0 the distribution is nearly symmetric for suitably chosen photon polarisation. For a PLC the convoluted differential cross section is for $m_0 = 50$ GeV in the backward region higher than that for a monochromatic unpolarized photon beam. For $m_0 = 200$ GeV it is always smaller.

The discussion of the background is postponed to a forthcoming paper. There will also be presented more detailed results including the influence of different polarizations of laser photons and converted electrons.

This work was supported by the German Federal Ministry for Research and Technology (BMBF) under contract number 05 7WZ91P (0).

REFERENCES

[1] H.E. Haber, G.L. Kane, *Phys. Rep.* **117**, 75 (1985).

[2] L.J. Hall, J. Polchinski, *Phys. Lett.* **152B**, 335 (1985); A. Bartl, W. Majerotto, B. Mösslacher, e^+e^- Collisions at 500 GeV, DESY 92-123 B, 641 (1992).

[3] I.F. Ginzburg, G.L. Kotkin, S.L. Panfil, V.G. Serbo, V.I. Telnov, *Nucl. Inst.* **219**, 5 (1984); D.L. Borden, D.A. Bauer, D.O. Caldwell, *Phys. Rev.* **D48**, 4018 (1993); D.L. Borden, D.A. Bauer, D.O. Caldwell, SLAC-PUB-5715, 1992 (unpublished), UCSB-HEP-92-01, 1992 (unpublished); F. Cuypers, G.J. van Oldenborgh, R. Rückl, *Nucl. Phys.* **B383**, 45 (1992); F. Cuypers, G.J. van Oldenborgh, R. Rückl, MPI-Ph/93-70, LMU-93/12. M. Baillargeon, G. Bélanger, F. Boudjema, ENSLAPP-A-473/94.